International Forum on Aeroelasticity and Structural Dynamics
IFASD 2017
25-28 June 2017 Como, Italy

PASSIVE GUST LOADS ALLEVIATION IN A TRUSS-BRACED WING USING INTEGRATED DAMPERS

Christopher P. Szczyglowski[1], Simon A. Neild[1], Brano Titurus[1], Jason Z. Jiang[1], Jonathan E. Cooper[1], Etienne Coetzee[2]

[1]Faculty of Engineering
University of Bristol
Bristol, BS8 1TR, United Kingdom
christopher.szczyglowski@bristol.ac.uk

[2]Airbus
Filton, Bristol, BS34 7PA, United Kingdom

Keywords: truss-braced wing, discrete gust, loads alleviation, passive, dampers.

Abstract: Gust load cases tend to be critical for sizing the wing components and therefore methods of gust loads alleviation are necessary in order to reduce the overall weight of the wing structure. In this paper a method of gust loads alleviation for a truss-braced wing will be introduced which uses linear, rotational, viscous dampers co-located at the hinge joints connecting the truss structure to the wing to provide damping and thereby loads relief to the stress levels during a "1-cosine" gust. The aeroelastic model is based on the NASA/Boeing SUGAR VOLT truss-braced wing and MSC.Nastran is used throughout the study to compute the gust response. It is found that large values of torsional viscous damping coefficient are required in order to provide moderate loads relief across the wing. Furthermore, it is found that a damper placed at the strut-fuselage joint is more beneficial than a damper located at the strut-wing joint due to its consistent performance across a range of gusts.

1 INTRODUCTION

There has been much research in recent years in the use of more energy efficient aircraft configurations that will meet the environmental performance requirements required by initiatives such as Vision 2020 and Flight Path 2050. One solution is the implementation of new aircraft concepts that can provide a step change in performance over the current commercial airliner design. One such concept is the Truss-Braced Wing (TBW) aircraft; originally championed by Hurel Dubois during the 1940s [1] it has since become the subject of a major study conducted by NASA and Boeing under the name Subsonic Ultra Green Aircraft Research (SUGAR) [2].

A strut-braced wing provides many benefits over a traditional cantilever design. Firstly, the loads alleviation provided by the strut means that the inboard wing section can have a reduced chord and thickness compared to an equivalent cantilever wing. The strut also allows a larger wingspan to be achieved which, when combined with the reduced chord, results in an increased aspect ratio providing an overall aerodynamic benefit, however, the interference drag associated with the truss structure can have a detrimental effect on performance if it is not properly designed. Despite this, numerous studies have shown, combining all of these effects can provide a significant reduction on take-off weight and fuel burn [3–9].

Preliminary sizing analysis carried out as part of the SUGAR project [9, 10] has shown that gust loads and other aeroelastic phenomena such as flutter are the main design drivers which size the structural components in a truss-braced wing. Traditionally, reducing gust loads or increasing the flutter speed would require specific tailoring of the stiffness and/or mass properties of the structure, which would lead to an inevitable increase in mass.

An alternative strategy is to operate aerodynamic control surfaces using control laws in order to modify the wing aerodynamic forces in such a way that the wing gust response is alleviated [11]. This method is now commonplace within the aerospace industry and many commerical aircraft operate this system. An extension to this method which has received an increased level of research in recent years is the use of the wing tip to provide loads alleviation. Castrichini *et al.* [12] investigated a folding wing tip device which could reduce static and dynamic loads by careful design on the hinge stiffness and hinge angle. Similarly, a Variable Geometry Raked Wing Tip [13] has been proposed as part of the SUGAR project which utilises the sweep of the wing tip device to provide a restoring torque to the wing in order to counteract aerodynamic moments and provide roll control. This device has also been incorporated into a multi-disciplinary optimisation scheme by Mallik *et al.* [14] and it was found that such a device allowed the operation of TBW configurations that otherwise would have failed the flutter constraints.

In this paper a novel approach to gust loads alleviation is proposed which utilises a damper integrated into the truss structure to provide additional damping and thereby loads relief during dynamic responses. The truss introduces several joint locations where a two-terminal device such as a damper, a spring-damper or even a more elaborate device such as a tuned-inerter-damper [15] could be utilised to reduce dynamic loads or alleviate flutter. This study will investigate the ability of a rotational viscous damper located at one of the truss hinge joints to reduce the maximum sectional stresses throughout a discrete ”1-cosine” gust. A damper device is considered to be the simplest possible dynamic device and will act as a suitable baseline for any further studies.

This paper begins with a description of the aeroelastic model and the method for modelling the dampers, as well as an explanation for the different joint connections and boundary conditions used throughout the analysis, this is carried out using MSC.Nastran [16]. Next, the normal modes of the TBW model are determined before performing a gust analysis on the TBW model in the clean configuration (i.e. without any dampers). Once the baseline gust response of the model has been determined the gust response is found for two different damper locations and a variety of damping coefficients. Finally, the findings of the study are discussed and conclusions are drawn in the final section as well as suggestions for further work.

2 TRUSS-BRACED WING AEROELASTIC MODEL

2.1 Structural Modelling

Figure 2 (a) shows the structural model used for the analysis. The TBW model is based on the NASA/Boeing SUGAR VOLT aircraft [10] however, due to the initial focus of the study only the wing is considered. The structural model has three parts: the wing, primary strut and the jury-strut. Each part of the structure is modelled as a beam, an appropriate modelling assumption due to the high-aspect ratio design of the SUGAR VOLT wing, with stiffness and mass properties derived from [10] and [17]. The wing, strut and jury-strut are composed of 35, 18 and 9 beam elements respectively and the model has 1194 degrees of freedom.

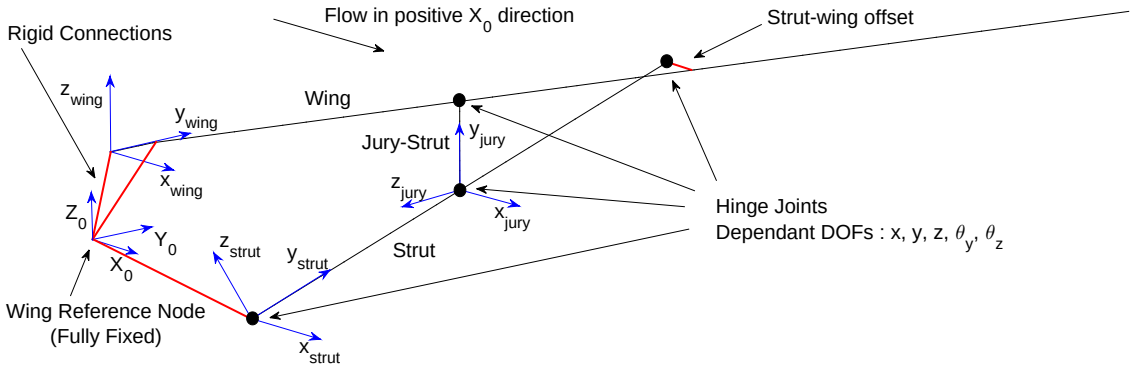

Figure 1: Schematic of the TBW model.

The topology of the truss-structure matches the SUGAR VOLT wing and is defined using the data in Figures 3.1-3.3 of [10]. The strut attaches to the wing at approximately 58% wing semi-span and is offset from the beam-line towards the leading edge in order to provide a passive loads alleviation benefit [8]. The jury-strut root position is at the mid-point of the primary strut and extends vertically upwards, meeting the wing at 35% of the wing semi-span.

For this study it is assumed that the truss-structure is connected to the wing via simple hinge joints. These joints allow rotation about the local beam x-axis whilst all other Degrees Of Freedom (DOF) are dependant. This means that out-of-plane bending moments are not transferred across these joints however, all forces as well as in-plane and torque moments are transmitted. Figure 1 describes the model orientation and the dependent DOF at each connection point. The wing model is fully-fixed at the wing reference node and additional boundary conditions are enforced at the wing root, wing kink and the strut-root via the use of RBE2 elements. The wing reference node lies on the centre line of the fuselage and is aligned with the Nastran basic coordinate system.

2.2 Aerodynamic Modelling

Figure 2 (b) shows the aerodynamic mesh for the TBW. The aerodynamic forces and moments are calculated using the Double Lattice Method (DLM) provided as part of the aeroelastic solution sequences in MSC.Nastran. The doublet lattice method is based on linear unsteady potential flow theory, meaning that the aerodynamic forces are only valid for inviscid, irrotational, incompressible and attached flow, subject to small angles of attack or side-slip. Despite these limitations the DLM aerodynamics are considered to be appropriate in order to obtain an understanding of the general wing response to a discrete gust.

For this study the aerodynamic coordinate system is aligned with the basic coordinate system (X_0, Y_0, Z_0) and the wing and the primary strut are modelled as aerodynamic surfaces, in keeping with the assumptions of the SUGAR VOLT wing model. As the model comprises only the half-wing a symmetry condition is applied in the X-Z plane in order to obtain the correct spanwise distribution of the aerodynamic forces. A surface spline is used to connect the aerodynamic mesh to the structural grid nodes and transfer all forces and displacements. The aerodynamic mesh comprises 1010 aerodynamic panels with 900 in the wing 110 in the primary strut. Each panel is approximately 0.25m wide (Y_0 direction) and 0.32m long (X_0 direction).

One deviation from the SUGAR VOLT model is that for this study the primary-strut has a

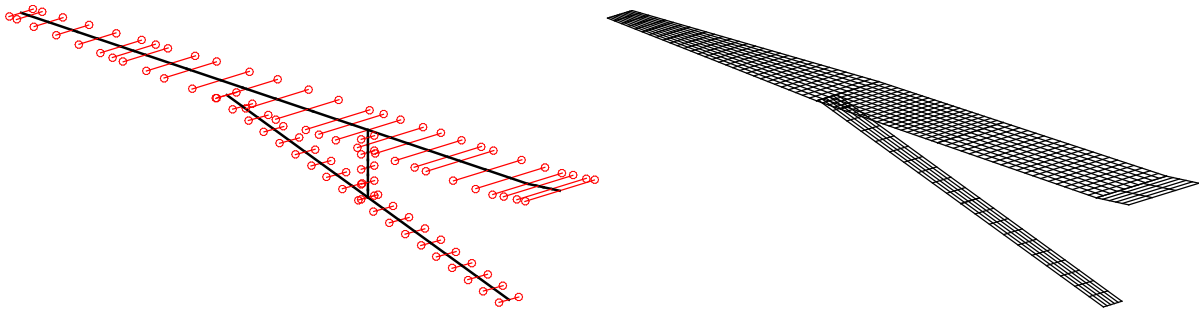

(a) Structural model (b) Aerodynamic model

Figure 2: Truss-braced wing structural and aerodynamic model.

constant chord length, as opposed to the distinctive bow-tie shape of the SUGAR VOLT primary strut, this is done in order to maintain the simplicity of the model. The chord value for the primary strut is based on the average of the SUGAR VOLT values.

2.3 Damper Modelling

To maintain simplicity the dampers are modelled as simple dashpot dampers generating linear, viscous damping. The dampers are rotational devices meaning that they provide a moment proportional to the relative angular velocity of the two terminals of the device.

$$M_{damper} = c\big(\dot{\theta}_A - \dot{\theta}_B\big) \tag{1}$$

where $\dot{\theta}_A$ is the angular velocity at the master node, $\dot{\theta}_B$ is the angular velocity at the slave node, c is the torsional viscous damping coefficient and M_{damper} is the moment generated by the damper. The dampers are included in the structural model as CBUSH elements [18].

3 EIGENANALYSIS

As the aeroelastic solution sequences in MSC.Nastran are based on a modal approach [16] it is important to have an understanding of the modeshapes and associated natural frequencies of the wing structure. Nastran Solution 103 was used to obtain the normal modes of the wing model in the frequency range $[0 : 30]$ Hz and in total 18 modes were found. A selection of these modes are shown in Figure 3; these modes feature heavily in the wing gust response and so have been included here for completeness.

The eigenanalysis revealed that the lower frequency modes are dominated by wing outboard bending and that the truss elements show very little participation, however, as the frequency increases the strut and jury-strut begin to feature more strongly. The modeshapes in Figures 3 (c) and (d) exhibit significant rotation about the hinge positions, therefore if these modes participate significantly in the gust response then a rotational damper placed at one of these locations could provide extra damping to the structure.

4 ”1-COSINE” GUST RESPONSE ANALYSIS

Nastran Solution 146 is used to determine the wing response to a discrete ”1-cosine” gust. As the unsteady aerodynamic forces are defined in terms of reduced frequency it is convenient to

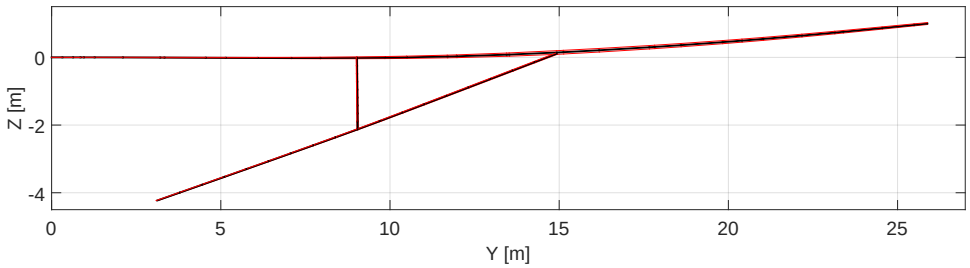

(a) First wing bending mode at 1.83Hz (Mode 1).

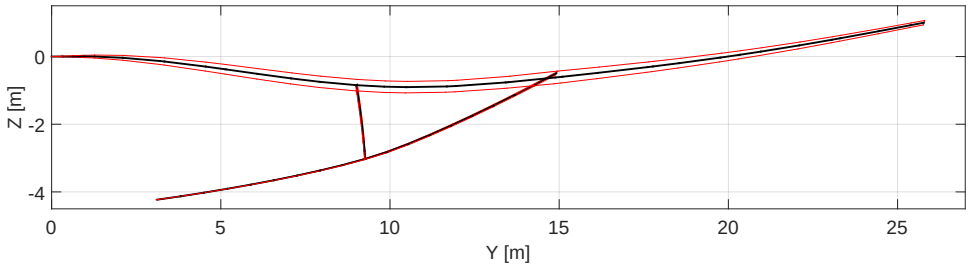

(b) Global bending mode at 2.83Hz (Mode 3).

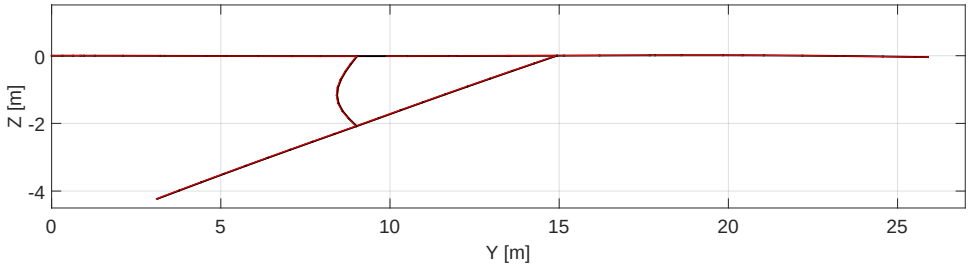

(c) Jury-strut bending mode at 8.03Hz (Mode 6).

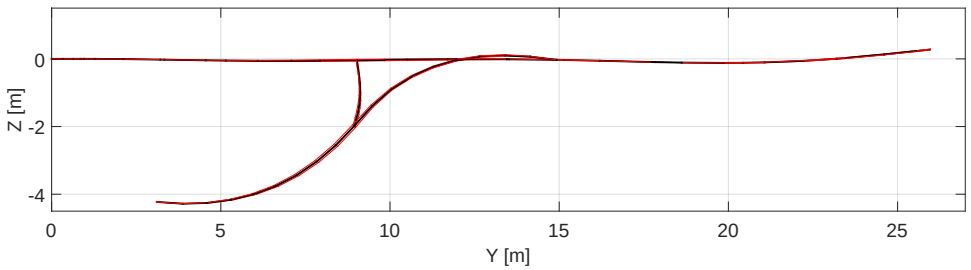

(d) Strut bending mode at 9.72Hz (Mode 8).

Figure 3: Truss-braced wing modeshapes. Black denotes the deflected shape of the beam elements and red is the outline of the TBW planfrom for this deflected shape.

compute the response in the frequency domain using modal coordinates. The generic aeroelastic equation of motion for dynamic aerolasticty in [16] is given by

$$\big[-M_{hh}\omega^2 + iB_{hh}\omega + (1+ig)K_{hh} - \frac{1}{2}V^2 Q_{hh}(m,k)\big]\{q_h\} = \{P(\omega)\} \tag{2}$$

where ω is the excitation frequency, M_{hh} is the modal mass matrix, B_{hh} is the modal damping matrix, g is the structural damping parameter, K_{hh} is the modal stiffness matrix, V is the aircraft forward velocity and Q_{hh} is the matrix of aerodynamic forces which is a function of reduced

frequency (k) and Mach number (m), q_h are the modal coordinates and $P(\omega)$ is the applied load defined as a function of excitation frequency.

The terms on the left-hand side of Equation 2 are determined automatically by MSC.Nastran based on the model definition and aircraft velocity for a set of user-defined values of reduced frequency and Mach number. The inclusion of a gust in Equation 2 requires the frequency variation of the gust to be specified, however, as the certification requirements define the gust profile in the time domain [19] it is more convenient to first define the gust as a time varying signal and then transform this into the frequency domain using the Fourier Transform. This process is entirely automated within MSC.Nastran and does not require any additional computation once the time domain gust signal has been defined.

Using the "1-cosine" definition of a discrete gust yields

$$w_g(t) = \frac{U_{ds}}{2}\big[1 - cos(\frac{\pi V t}{H})\big], \tag{3}$$

which is taken directly from the certification requirements for large aircraft, Certification Specification 25 (CS-25), as provided by EASA [19]. Here w_g is the gust vertical velocity, H is the gust gradient (distance to reach the peak gust velocity), V is the aircraft forward velocity in TAS and U_{ds} is the gust design velocity, defined as

$$U_{ds} = U_{ref} F_g \big(\frac{H}{106.17}\big)^{\frac{1}{6}}, \tag{4}$$

where F_g is the flight load alleviation factor and U_{ref} is the reference gust velocity in EAS, varied linearly from 13.4m/s EAS at 15,000ft to 7.9m/s EAS at 50,000ft as specified in CS-25. Assuming that the aircraft is operating at a cruise altitude and Mach number of 36,000ft and M=0.75 respectively [10], yielding a gust reference velocity of 10.12m/s EAS and a flight load alleviation factor 0.98. Furthermore, a frequency resolution of Δf = 0.005Hz is selected and 6000 frequency increments are defined in order to cover the frequency range $[0 : 30]$ Hz.

Finally, it is important to note that as the wing reference node is fully-fixed, the rigid body modes will not participate in the gust response. This will of course have a significant effect on the participation of the flexible modes, however, as this is a preliminary investigation this simple approach is deemed satisfactory.

5 GUST RESPONSE OF THE TRUSS-BRACED WING

Before the loads alleviation of the damper can be assessed the baseline gust response of the TBW must be established. Three gust gradients are considered, 9m, 53m and 107m, in order to understand the effect that the different frequency content of these gusts will have on the modal response of the wing (Figure 4).

From Figure 5 it is clear that the wing response across all of the gusts is dominated by modes 1 and 3. This is because the natural frequencies of these modes are within the frequency bandwidth of each of the gusts and will therefore feature strongly. However, it is interesting to note that modes 6 and 8, which are jury-strut/strut dominated, do not feature significantly in the 53m and 107m gusts as these higher frequency modes fall outside the bandwidth of the longer gusts. For the shorter gusts the frequency bandwidth is much higher and therefore a larger number of modes feature in the response, this will lead to additional parts of the structure being excited which will have a knock-on effect on the stresses throughout the wing.

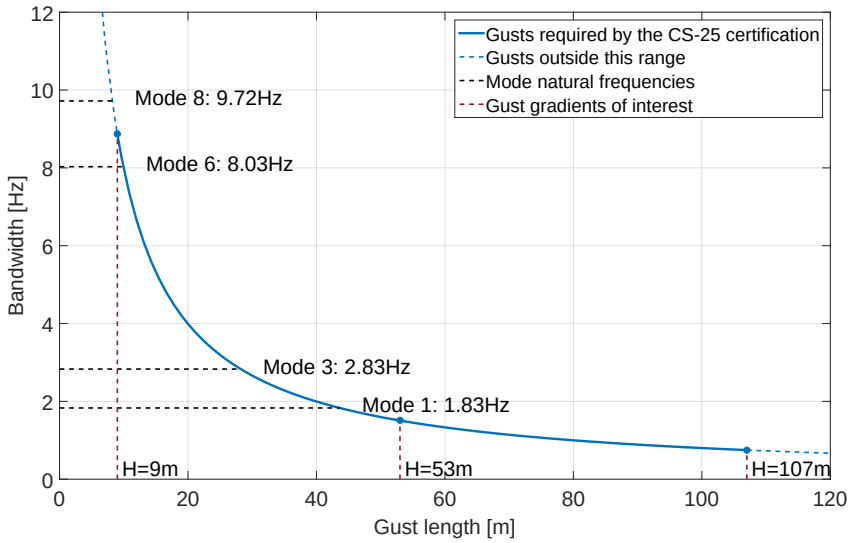

Figure 4: Gust bandwidth as a function of gust gradient.

The direct stress distribution is a key consideration during gust load cases as these stresses tend to be critical for sizing the wing box components. Figure 6 shows the maximum and minimum stress envelopes for the three gust gradients considered. By examining Figure 6 it is clear that the shape of the stress distribution is drastically different to that of a cantilevered wing. For a TBW configuration the strut and jury-strut transmit considerable loads into the wing structure, especially in terms of in-plane shear and axial forces, which causes significant loading inboard of the primary strut attachment point. Also, as the truss elements have a large axial stiffness the truss attachment points undergo very little deflection meaning that much of the bending stress is a result of high curvatures between these attachments points. This leads to the pinched stress distribution seen in Figure 6.

This non-standard stress distribution makes the process of identifying a worst-case gust much more difficult as it is not immediately clear where the highest stress levels will occur because different gusts excite different parts of the structure, whereas for a cantilever wing the highest stresses will generally occur at the wing root. The maximum stress levels inboard of the strut occur for the longer gusts as the wing response is dominated by modes 1 and 3 which cause significant bending and axial stresses along the wing, especially mode 3 which is a global bending mode. The outboard portion of the wing experiences the most severe stress as a result of the shorter 9m gust, this is due to the presence of localised outboard bending modes which are not captured by the reduced bandwidth of the longer gusts.

6 GUST RESPONSE USING EMBEDDED DAMPERS

In the previous section it was observed that for certain modeshapes the truss elements rotate about their hinge connections and it was hypothesised that this motion could be exploited by a damper in order to reduce peak stress levels during a gust. To test this two locations have been identified as suitable candidates for dampers: Location A is the hinge joint at the strut-wing juncture and Location B is the hinge joint at the strut-fuselage connection (Figure 7).

The gust response of the TBW model is determined for the 9m and 53m gusts as these were observed to be the critical cases with regards to the direct stress distribution over the wing. Three values of the torsional viscous damping coefficient are tested, 100, 10,000 and 100,000$Nm/rads^{-1}$,

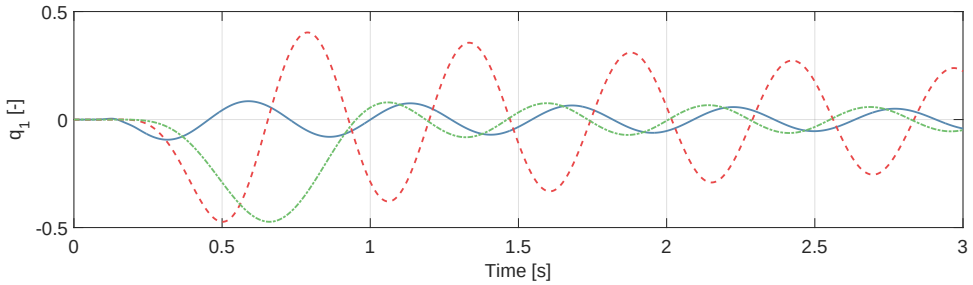

(a) Mode 1.

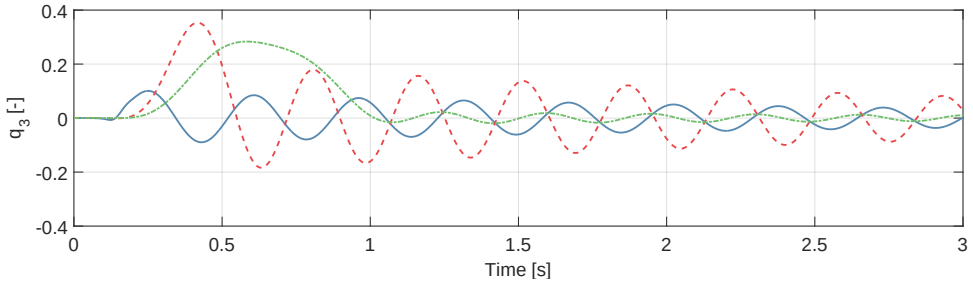

(b) Mode 3.

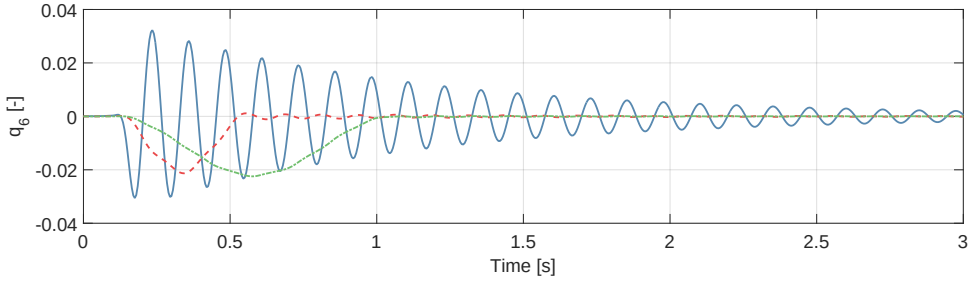

(c) Mode 6.

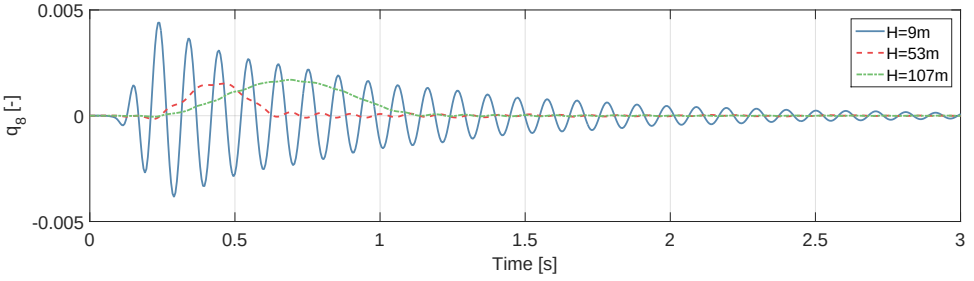

(d) Mode 8.

Figure 5: Modal coordinates for gust gradients H=9m, H=53m and H=107m

in order to assess the magnitude of damping coefficient required to provided loads relief to the wing. For each gust analysis only one damper is active at a time so as to determine whether a particular single location is superior in terms of providing loads relief.

Figure 8 shows the change in maximum and minimum stress due to the effects of the damper at the two hinge locations. For the maximum stress plots a negative value of $\Delta\sigma$ means the damper has a benefit on the stress levels, whereas for the minimum stress plots a positive value of $\Delta\sigma$ denotes a benefit to the stress levels.

Examining the data for the 9m gust (panels (a) and (b) of Figure 8) it is evident that a large damping coefficient is required to influence the stress levels in the wing. For a damping coefficient of $100Nm/rads^{-1}$ there is a negligible change in wing stresses to that experienced

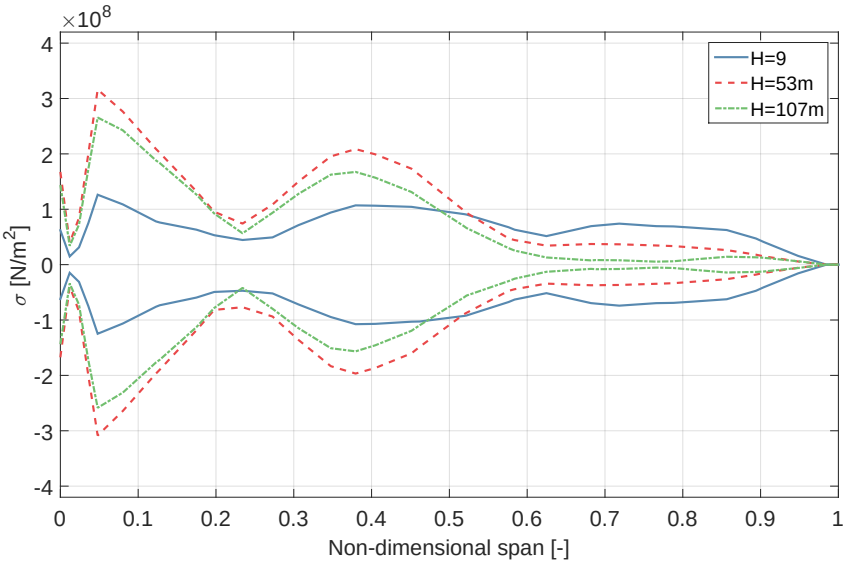

Figure 6: Wing direct stress envelope for gust gradients H=9m, H=53m and H=107m.

when no damper is fitted. Increasing c to 10,000$Nm/rads^{-1}$ provides a peak reduction of $5 \times 10^6 N/m^2$ at approximately 85% of the semi-span using a device at Location B and increasing c further to 100,000$Nm/rads^{-1}$ yields a three fold reduction in stress of $15 \times 10^6 N/m^2$ at the same spanwise location.

The 9m gust results show that a damper at either location is capable of providing some loads relief to the wing, with the damper at Location B providing a larger reduction in stress for a given value of damping coefficient for the majority of locations, the exception being at the wing root position where the strut-wing joint damper is superior. However, a damper placed at the strut-wing joint can cause an increase in the absolute values of stress along the wing which is clearly not desirable. This is also the case for the strut-fuselage damper, however the effect is much reduced. In general, a large damping coefficient yields a larger reduction in stress levels, however, as previously mentioned this can lead to an increase in stress for some parts of the wing for a device at Location A.

The reduction in minimum stress levels for the 9m gust follows the same broad trends as the maximum stresses: the strut-fuselage damper has the best performance across the span with the exception of the wing root stresses where the strut-wing dampers provides a better reduction

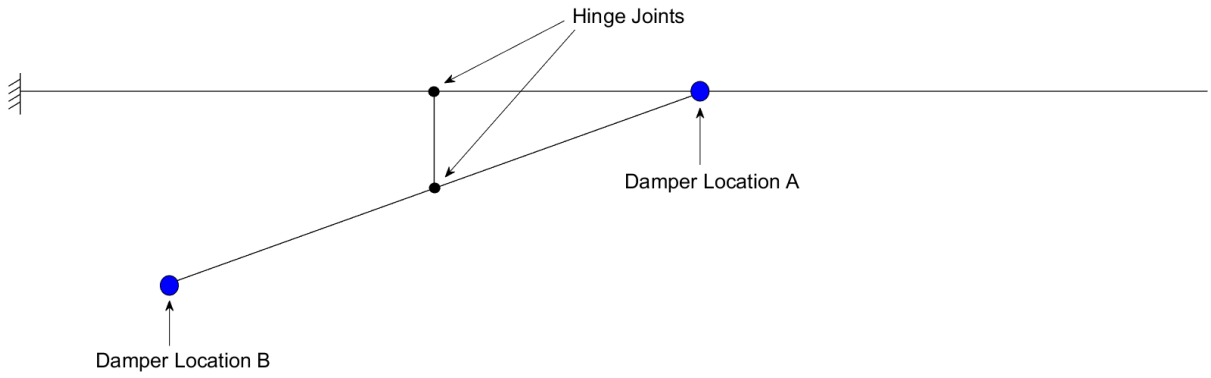

Figure 7: Side view of the TBW with the damper positions annotated.

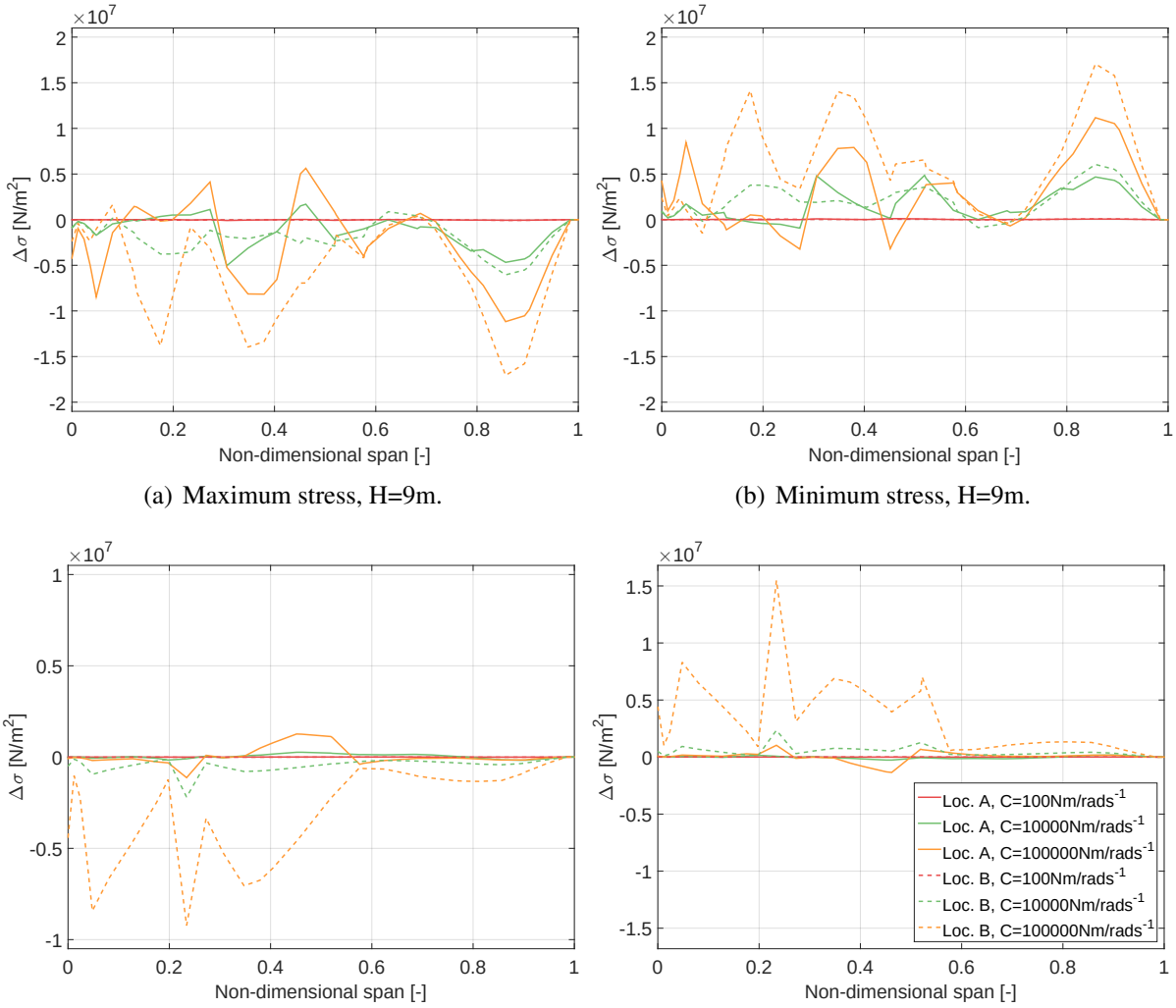

(a) Maximum stress, H=9m.

(b) Minimum stress, H=9m.

(c) Maximum stress, H=53m.

(d) Minimum stress, H=53m.

Figure 8: Change in stress across the wing for the two damper locations and torsional viscous damping coefficient c=[100, 10000, 100000]$Nm/rads^{-1}$ for gust gradients H=9m (a) & (b) and H=53m (c) & (d)

and the stress can be made worse by a damper at the strut-wing joint that has a high damping coefficient. Additionally, the low damping case (c = 100$Nm/rads^{-1}$) has a negligible effect on the stress levels.

With regards to the 53m gust there is a clear difference between device location and damping coefficient value. Firstly, a damper located at the strut-fuselage joint (Location B) is capable of delivering a larger reduction in wing stresses than an equivalent damper placed at Location A. This is because the hinge joint at Location B experiences greater angular velocities during the 53m gust than the joint at Location A (Figure 9), therefore the moment produced by the damper will be greater in magnitude and have a more significant effect on the wing stresses. Secondly, it seems that only the highest value of damping coefficient (c = 100,000$Nm/rads^{-1}$) has any appreciable effect. Again, Figure 9 shows that this is because the magnitude of the angular velocities at both hinge positions is lower for the 53m than for the 9m gust, therefore a larger value of damping coefficient is required to achieve the same moment from the damper and hence the same reduction in stresses.

For the 53m gust the wing stress levels inboard of the strut joint are more sensitive to the moment produced by the damper whereas for the 9m gust the greatest reduction in stresses

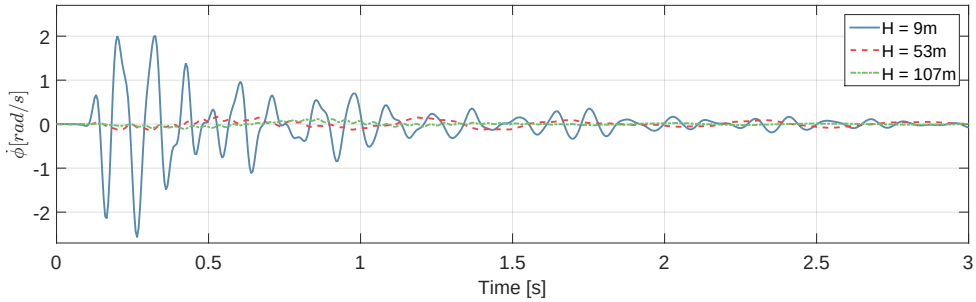

(a) Relative angular velocity at the strut-wing hinge joint.

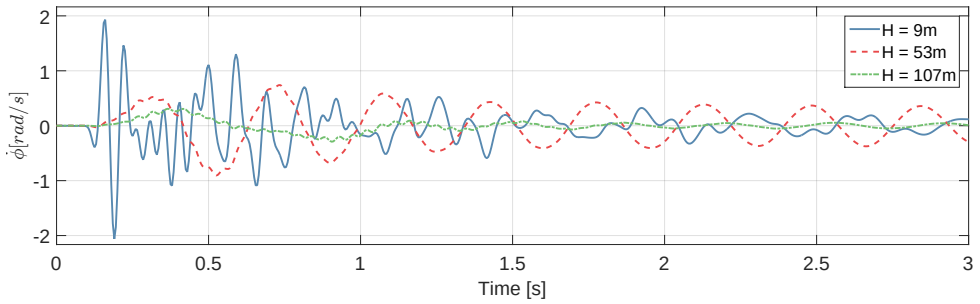

(b) Relative angular velocity at the strut-fuselage hinge joint.

Figure 9: Relative angular velocity between the damper terminals at (a) Location A and (b) Location B.

is seen in the outboard portion of the wing. These findings compliment one another nicely as both the maximum and minimum stresses inboard of the strut joint were due to the 53m gust and stresses in the outboard section were due to the 9m gust. Therefore, by combining these two schemes, there is the potential to reduce the maximum stress levels across the entire span of the wing. It is worth mentioning that the loads alleviation provided by the dampers is small in comparison to the absolute values of the wing stresses. Furthermore, to achieve these moderate reductions in stress levels a high value of damping coefficient is required which may be difficult to implement physically given the limited space available within the wing torque box. A possible alternative could be to investigate the use of the jury-strut as a translational device for loads alleviation. This could be in the form of a spring and damper in parallel which would then act to modify the wing response in order to reduce the participation of the low frequency modes which contribute the most to the wing stresses.

7 CONCLUSION

This paper has presented a novel method for gust loads alleviation in a truss-braced wing based on using rotational dampers co-located with the strut hinge joints to impart damping into the wing structure. It has been shown that such a scheme can provide moderate reductions in the stress levels in the wing, although this requires very large damping coefficients. Two hinge locations were tested and it was found that a damper located at the strut-fuselage joint generally provided a greater reduction in wing stresses, with the exception of the wing root where the strut-wing location was superior. It is suggested that implementing a damper at both locations simultaneously has the potential to provide further loads alleviation compared to the dampers acting separately.

Additionally, a discussion on the ”1-cosine” gust response of a truss-braced wing has been provided and it was found that the frequency content of the gust has an important role in determining the worst case stress levels along the wing. For the wing section inboard of the strut

attachment point the 53m gust was critical, however the reduced stiffness of the outboard portion of the wing meant that the 9m gust was critical due to the presence of localised bending modes.

Future work will focus on further exploiting the truss topology to introduce loads alleviation devices which utilise the relative motion of the structure, such as a translational device placed in the jury-strut or multiple rotational devices placed at the hinge joints. Furthermore, the analysis will be expanded to include modelling of continuous turbulence and the aeroelastic model will be extended to a full aircraft model, allowing the participation of the rigid body modes to be included which may affect the suitability of a loads alleviation device.

ACKNOWLEDGMENTS

This research is funded by UK Aerospace Technology Institute Agile Wing Integration (AWI) project (TSB-113041). Simon A. Neild is supported by an EPSRC Fellowship (EP/K005375/1), Jason Z. Jiang is supported by an EPSRC grant (EP/P013456/1) and Jonathan E. Cooper holds a Royal Academy of Engineering Chair.

8 REFERENCES

[1] (1952). Hurel dubois transports: Progress with the hd-31 and 32: The hd-45 jet project. *Flight and Aircraft Engineer: Official Organ of the Royal Aero Club*, 2288(62), 676–677.

[2] Bradley, M. K. and Droney, C. K. (2011). Subsonic ultra green aircraft research: Phase i final report. Tech. rep., NASA, CR-2011-216847.

[3] Park, P. H. (1980). Fuel consumption of a strutted vs cantilever-winged short-haul transport with aeroelastic considerations. *Journal of Aircraft*, 17(12), 856–860.

[4] Turriziani, R., Lovell, W., Martin, G., et al. (1980). Preliminary design characteristics of a subsonic business jet concept employing an aspect ratio 25 strut braced wing. Tech. rep., 1981-0002505.

[5] Smith, P. M., DeYoung, J., Lovell, W. A., et al. (1981). A study of high-altitude manned research aircraft employing strut-braced wings of high-aspect-ratio.

[6] Jobe, C. E., Kulfani, R. M., and Vachal, J. D. (1979). Wing planforms for large military transports. *Journal of Aircraft*, 16(7), 425–432.

[7] Carrier, G., Atinault, O., Dequand, S., et al. (2012). Investigation of a strut-braced wing configuration for future commercial transport. In *28th Congress of the International Council of the Aeronautical Sciences*. ICAS Bonn, pp. 2012–1.

[8] Bhatia, M., Kapania, R. K., and Haftka, R. T. (2012). Structural and aeroelastic characteristics of truss-braced wings: A parametric study. *Journal of Aircraft*, 49(1), 302–310.

[9] Mallik, W., Kapania, R. K., and Schetz, J. A. (2015). Effect of flutter on the multidisciplinary design optimization of truss-braced-wing aircraft. *Journal of Aircraft*, 52(6), 1858–1872.

[10] Bradley, M. K., Droney, C. K., and Allen, T. J. (2015). Subsonic ultra green aircraft research. phase ii-volume i; truss braced wing design exploration. Tech. rep., NASA, CR-2015-218704.

[11] Karpel, M. (1982). Design for active flutter suppression and gust alleviation using state-space aeroelastic modeling. *Journal of Aircraft*, 19(3), 221–227.

[12] Castrichini, A., Siddaramaiah, V. H., Calderon, D., et al. (2017). Preliminary investigation of use of flexible folding wing tips for static and dynamic load alleviation. *The Aeronautical Journal*, 121(1235), 73–94.

[13] White, E. V., Kapania, R. K., and Joshi, S. (2015). Novel control effectors for truss braced wing. Tech. rep., CR2015-218792.

[14] Mallik, W., Kapania, R. K., and Schetz, J. A. (2016). Aeroelastic applications of a variable-geometry raked wingtip. *Journal of Aircraft*, 1–13.

[15] Lazar, I., Neild, S., and Wagg, D. (2014). Using an inerter-based device for structural vibration suppression. *Earthquake Engineering & Structural Dynamics*, 43(8), 1129–1147.

[16] Rodden, W. P. and Johnson, E. H. (1994). *MSC/NASTRAN aeroelastic analysis: user's guide; Version 68*. MacNeal-Schwendler Corporation.

[17] Su, W. (2017). Nonlinear aeroelastic analysis of aircraft with strut-braced highly flexible wings. In *58th AIAA/ASCE/AHS/ASC Structures, Structural Dynamics, and Materials Conference*. p. 1351.

[18] McCormick, C. W. (1983). *MSC/NASTRAN User's Manual: MSC/NASTRAN Version 63*. MacNeal-Schwendler Corporation.

[19] (2003). *CS-25 Certification Specifications for Large Aeroplanes*. European Aviation Safety Agency (EASA).

COPYRIGHT STATEMENT